T–T Base Mismatches Enhance Drug Binding at the Branch Site in a Four-Arm DNA Junction

Min Zhong, Michael S. Rashes, Luis A. Marky, and Neville R. Kallenbach*

Department of Chemistry, New York University, New York, New York 10003

Received April 10, 1992; Revised Manuscript Received June 2, 1992

ABSTRACT: Base mismatches—non Watson–Crick pairing between bases—can arise in duplex DNA as a consequence of mutational events or by recombination. In a duplex, the sequence of the two bases involved, and those flanking the site of mismatch, determines the local structure and extent of destabilization of the helix. Base mismatches can arise also in recombination of nonhomologous strands, and their occurrence in Holliday recombination intermediates can influence the outcome of general or specialized recombination events. We have previously reported that the branch site in a DNA junction can interact selectively with a variety of ligands. Here we describe the thermodynamics of junctions containing T–T mismatches flanking the branch and show that these structures bind methidium and other intercalators with higher affinity than junctions lacking mismatches.

The availability of stable oligonucleotide models for branched DNA molecules, including analogs of Holliday junctions that might exist as intermediates during recombination, has made it possible to establish important features of these structures, including their thermodynamic parameters, ability to bind drugs, and the role of sequence in determining their conformation [see Lu et al. (1992a) for a review]. Results of experiments on four-arm junctions have led to definition of their overall configuration, which in the presence of Mg^{2+} or high Na^+ concentrations is thought to assume a specific fold with two adjacent arms stacked over each other to form an overall X-shaped structure based on fluorescence energy transfer data (von Kitzing et al., 1990). Some caution concerning the interpretation of fluorescence energy transfer data on end-labeled junctions needs to be exercised, however (Cooper & Hagerman, 1990). The branch site in DNA junctions has unusual binding properties for a variety of ligands (Guo et al., 1989, 1990). Intercalative agents including ethidium and chloroquine, porphyrins, and the dye Stains-All have been shown to interact preferentially at the branch in four-arm junctions (Lu et al., 1992b).

The structural (Kneale et al., 1985) and thermodynamic (Tibanyenda et al., 1983; Aboul-Ela et al., 1985; Werntges et al., 1986) properties of base mismatches have been studied in the context of duplex DNA using oligonucleotide models. Because of their bearing on mutagenesis, DNA repair mechanisms, and hybridization experiments, defining these states of a duplex is important. Since recombination of nonhomologous strands can generate Holliday intermediates that contain mismatches, the question of how mismatches affect the structure and stability of DNA junctions is also of interest in both general and specialized recombination (Nash & Robertson, 1989). A similar order of destabilization by different bases has been reported for mismatches flanking the branch site in four-arm junctions (Duckett & Lilley, 1991) as is found for mismatches in duplex DNA (Aboul-Ela et al., 1985; Werntges et al., 1986). For example, in both duplexes and junctions, G-containing mismatches tend to be the most stable and C-containing mismatches least stable. This implies (Duckett & Lilley, 1991) that these structures share common features, as anticipated from structural models that have been proposed for four-arm junctions (Cooper & Hagerman, 1987; von Kitzing et al., 1990). The branch site nevertheless has very different liganding properties from those of a duplex (Lu et al., 1992a). This prompted us to investigate the role of mismatches on the selectivity and affinity of drug interactions in junctions with mismatches flanking the branch. The model system we have chosen is the well-studied four-arm DNA junction J1, composed of the four complementing strands illustrated in Figure 1 (Kallenbach et al., 1983), together with the three mismatch-containing analogues, T2, T3, and the double mismatch T2T3, the sequences of which are shown in Figure 1. The junction T2 contains a T–T mismatch in the left arm of the model illustrated, due to replacement of A8 in strand 2 by T; T3 contains a similar T–T mismatch in the right arm of the junction, from replacement of A9 in arm 3 by T; and T2T3 has both of these T–T mismatches.

MATERIALS AND METHODS

(*a*) *Synthesis and Purification of Oligonucleotides.* Oligonucleotides used in this study were synthesized on an Applied Biosystems 391 automated DNA synthesizer, deprotected by routine phosphoramidite procedures (Caruthers, 1982), and purified by ion-exchange HPLC (Du Pont Zorbax Bio Series oligonucleotide column). 5′-Terminal labeling was achieved with bacteriophage T4 polynucleotide kinase (BRL) and [γ-^{32}P]ATP; the labeled strands were purified by PAGE. The concentration of strands in stock solutions was determined spectrophotometrically at 260 nm and 80 °C, using the molar extinction coefficients given in Table I.

(*b*) *Annealing Reactions.* These were carried out by mixing stoichiometric concentrations of the appropriate DNA strands in 50 mM Tris-HCl (pH 7.5) with 10 mM $MgCl_2$, heating at 90 °C for 2 min, cooling slowly to room temperature, and finally chilling to 4 °C. In each annealing reaction only one of the oligonucleotides was radioactively labeled, giving four different species for each junction.

(*c*) *Gel Electrophoresis.* Native gels contained 18% polyacrylamide (19:1 monomer/bis ratio), and the running buffer contained 40 mM Tris, 20 mM acetic acid, 1 mM $MgCl_2$ (pH 8.1), and 20 mM NaCl. Gels were run at 8 V/cm for 20 h, cooled by a circulating waterbath (4 °C), and exposed for 1 h without an intensifying screen. For denaturing gels, the products of cleavage reactions were taken up in formamide loading buffer, heated to 90 °C for 1 min, chilled to 0 °C, and

0006-2960/92/0431-8064$03.00/0

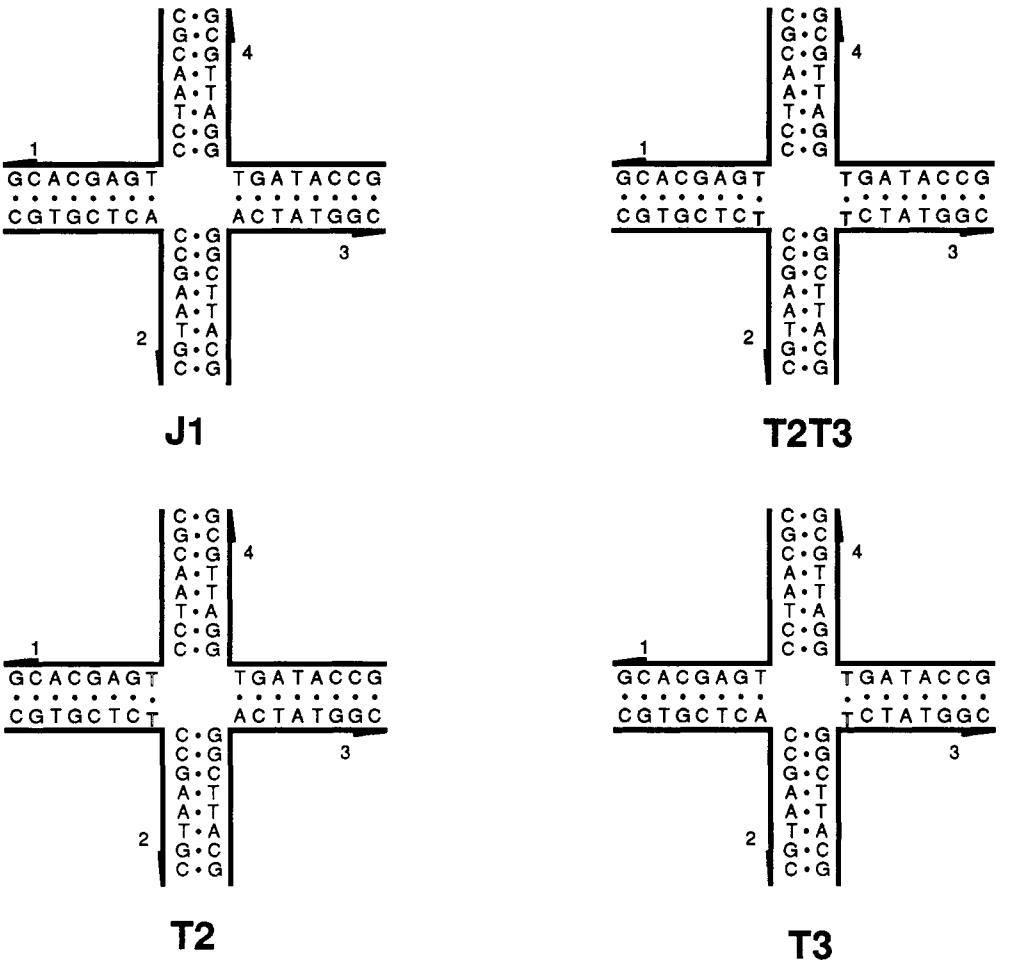

FIGURE 1: Sequences of the four synthetic DNA four-arm junctions used in this study. The junctions are shown schematically as a cross, and each consists of four 16-mer strands of DNA. The 3′ ends of the strands are indicated by half-arrowheads. The strand numbering indicated in this figure is used throughout the text.

Table I: Molar Extinction Coefficients of DNA Strands Used in This Study[a]

sequence	ϵ_{260nm} (mM^{-1} cm^{-1})	sequence	ϵ_{260nm} (mM^{-1} cm^{-1})
d(CGCAATCCTGAGCACG)	158	d(GCCATAGTGGATTGCG)	163
d(CGTGCTCACCGAATGC)	151	d(CGTGCTCTCCGAATGC)	147
d(GCATTCGGACTATGGC)	155	d(GCATTCGGTCTATGGC)	152

[a] The above values were measured with melting curves by extrapolation to 80 °C of the molar extinctions calculated using nearest-neighbor values of Cantor et al. (1970).

run on 20% polyacrylamide (19:1 monomer/bis ratio)/7 M urea gels for 2.5 h at 2000-V constant voltage (ca. 50 V/cm) and 40 °C. Gels were dried immediately on a vacuum drying apparatus (Hoefer) and exposed to X-film at −70 °C using a Du Pont Cronex Lightning Plus intensifying screen.

(*d*) *UV Melting Curves.* Absorbance vs temperature profiles (melting curves) for the junctions, at various strand concentrations in a 20 mM sodium cacodylate buffer containing 100 mM NaCl and 1 mM $MgCl_2$ (pH 7.0), were measured at 260 nm with a thermoelectrically controlled Perkin-Elmer 552 spectrophotometer interfaced to a PC-XT computer for acquisition and analysis of experimental data. The temperature was scanned at a heating rate of 1 °C/min. These melting curves allow us to measure the transition temperatures, T_m, the midpoints of the order–disorder transition of these DNA molecules, and to determine the associated van't Hoff thermodynamic parameters (Marky & Breslauer, 1987), with a two-state approximation to the helix–coil transition of each molecule. The application of this approximation to a branched molecule such as J1 has been discussed by Marky et al. (1987).

(*e*) *Differential Scanning Calorimetry.* The total heat of the helix–coil transition of each junction was measured directly with a Microcal MC-2 differential scanning calorimeter (DSC) interfaced to an IBM PC computer. A typical solution for these experiments contained 20 mM sodium cacodylate, 100 mM NaCl, and 1 mM $MgCl_2$ (pH 7.0) with a concentration of 0.46 mM (in strands) and was scanned from 0 to 85 °C at a heating rate of 45 °C/h (0.75 °C/min). The experiment was repeated with heating–cooling cycles to improve signal to noise and verify the complete reversibility of the transitions. A buffer alone was used as blank; a buffer vs buffer scan was subtracted from the sample scan and normalized for the heating rate. The area of the resulting curve is proportional to the transition heat, which, normalized for the number of moles, gives the transition enthalpy ($\Delta H°_{cal}$). These DSC curves also allow one to estimate the transition entropy ($\Delta S°_{cal}$) and free energy ($\Delta G°_{cal}$) from the area of a graph of $\Delta C_p/T$ vs T and the Gibbs equation, respectively.

(*f*) *MPE·Fe(II) Cleavage.* DNA samples (10 μM) were exposed to 10 μM Fe(II) and 10 μM MPE (van Dyke & Dervan, 1983a,b) in a buffer containing 10 mM Tris-HCl

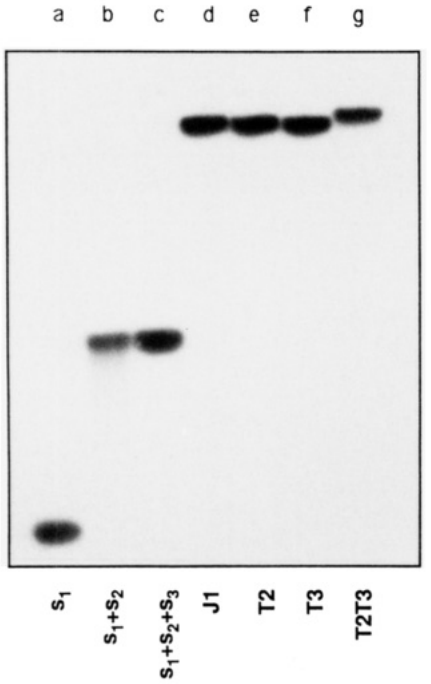

FIGURE 2: Polyacrylamide gel electrophoresis of oligodeoxynucleotide strands and mixtures. An autoradiogram of a native gel is shown, in which strand 1 of junctions is labeled and run alone or in combination with one, two, or three other cold strands in excess. The numbering convention refers to that of Figure 1. Note that the tetrameric junction migrates as a single well-defined band with lower mobility than monomer, dimer, or trimer.

(pH 7.5) with 50 mM NaCl and 10 mM $MgCl_2$ for 15 min at 4 °C, followed by addition of 4 mM DTT for 60 min, and the reaction was stopped by rapid ethanol precipitation and lyophilized.

(*g*) *Osmium Tetraoxide Modification.* Junctions (10 μM) were incubated with 1 mM osmium tetraoxide (OsO_4) and 3% pyridine in 50 mM Tris-HCl (pH 7.5) with 10 mM $MgCl_2$ at 4 °C for 15 min (Lilley & Palecek, 1984). Reactions were stopped by two sequential ethanol precipitations, and the mixes were lyophilized. The DNAs were cleaved at the site of reaction by treatment with 100 μL of 1 M piperidine at 90 °C for 30 min and lyophilized.

(*h*) *Diethyl Pyrocarbonate Modification.* Branched DNAs were modified by diethyl pyrocarbonate (DEPC) essentially as described by Herr (1985). DNAs (10 μM) were suspended in 10 μL of 50 mM Tris-HCl (pH 7.5) with 10 mM $MgCl_2$ and incubated with 1 μL of DEPC for 60 min at 4 °C. The reactions were terminated by two sequential rapid ethanol precipitations and then lyophilized. The DNAs were cleaved at the sites of DEPC modification by treatment with 100 μL of 1 M piperidine at 90 °C for 30 min and lyophilized.

(*i*) *Sequencing Reaction.* Purine-specific (A+G) sequencing ladders were generated from each 5′-^{32}P-labeled oligonucleotide using the piperidine–formate reaction (Maxam & Gilbert, 1980).

(*j*) *Densitometry.* Autoradiograms were scanned on a Hoefer GS300 densitometer, without baseline corrections.

RESULTS

(*a*) *Strands Containing T–T Mismatches Form Stoichiometric Junction Complexes.* To establish that the junctions containing mismatches form stable tetramers, the four strands corresponding to each junction were mixed and annealed in the presence of Mg^{2+} and subjected to native PAGE at 4 °C (Kallenbach et al., 1983). As shown in Figure 2, each tetramer migrates in native gels as a unique species with a mobility slower than the complexes formed by combinations of two or three strands. This is consistent with formation of a branched tetramer, as has been shown in the case of J1 itself (Kallenbach et al., 1983; Cooper & Hagerman, 1987). Species corresponding to duplexes, or triplexes, migrate more rapidly than the tetramer, which forms a single band in each case.

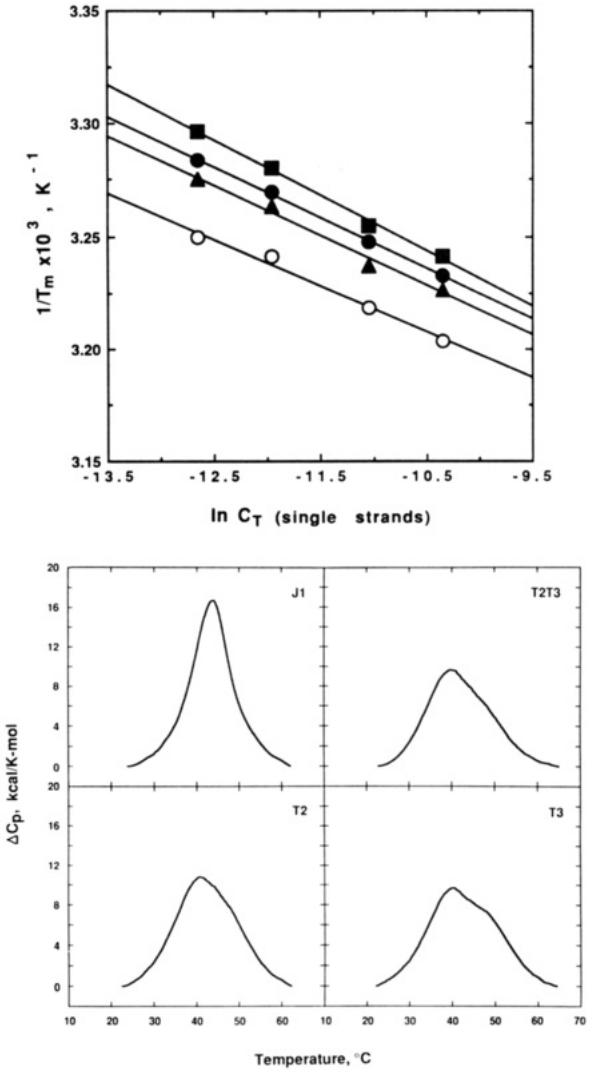

FIGURE 3: (A, top) Dependence of the transition temperature on strand concentration in 20 mM sodium cacodylate buffer containing 100 mM NaCl and 1 mM $MgCl_2$ (pH 7.0). The solid symbols represent junctions containing mismatches [(●) T3; (▲) T2; (■) T2T3], and the open circles (○) represent J1. (B, bottom) Differential heat absorption profiles for J1 and the mismatched junctions in 20 mM sodium cacodylate buffer containing 100 mM NaCl and 1 mM $MgCl_2$ (pH 7.0).

(*b*) *T–T Mismatches Destabilize Junctions.* The thermodynamics of forming a branch in DNA have been evaluated, by measuring the thermal unfolding of branched structures relative to duplexes corresponding to the four octamer arms (Marky et al., 1987), or two complementary 16-mer strands (Lu et al., 1992a,b). The free energy difference between a tetramer junction and two linear duplexes of the same length and sequence turns out to be the resultant of an unfavorable enthalpy change balanced by a favorable entropy. The former is easy to understand, since stacking interactions across the branch are broken relative to the intact duplexes. The origin of the favorable entropy is less obvious, since forming one tetramer by joining two duplexes should be entropically unfavorable. Our current hypothesis is that the favorable contributions arise from differential ion and water binding

Table II: Thermodynamic Parameters for Junction Formation at 20 °C[a]

	calorimetry					UV spectroscopy	
junction	T_m (°C)	$\Delta H°_{cal}$ (kcal/mol)	$\Delta\Delta H°_{cal}$	$\Delta G°$ (kcal/mol)	$T\Delta S°$ (kcal/mol)	$\Delta H°_{vH}$ (kcal/mol)	$\Delta\Delta H°_{vH}$ (kcal/mol)
J1	44	−210		−17	−193	−289	
T2	41	−191	19	−12	−179	−269	20
T3	40	−189	21	−13	−176	−265	24
T2T3	39	−168	42	−13	−155	−242	47

[a] All measurements were done in 20 mM sodium cacodylate buffer containing 100 mM NaCl and 1 mM $MgCl_2$ at pH 7.0. The calorimetric T_ms correspond to a total strand concentration of 460 μM. The $\Delta H°_{cal}$ values are averages of five determinations and are within ±3%; the $T\Delta S°$ values are within 5% experimental error. Spectroscopic $\Delta H°_{vH}$ values were determined from plots of $1/T_m$ vs ln C_T; these van't Hoff enthalpies are estimated to be within ±10% experimental error. The $\Delta\Delta H°_{cal}$ and $\Delta\Delta H°_{vH}$ values are relative to the corresponding enthalpies for J1.

betwen duplexes and a junction (Lu et al., 1992b). How a mismatch at the branch affects the stability of a junction and the underlying thermodynamics of junction formation is of interest.

The stability of junctions or duplexes formed from oligonucleotides depends on the strand concentration. Figure 3A compares this dependence for the intact junction J1 and the three mismatched species. No significant deviations from linear behavior are evident in any of these molecules, so that the apparent enthalpies can be estimated by applying a two-state model for the helix–coil transition (Marky & Breslauer, 1987). While the unfolding of J1 or similar branched structures is unlikely to be a two-state process, this procedure gives us a guide to the underlying thermodynamics. Table II summarizes the thermal transition midpoints (T_m) and van't Hoff enthalpy values for J1 and the mismatched junctions studied. These values are model dependent, as noted. Differential scanning calorimetry makes it possible to determine the enthalpy and other thermodynamic functions without recourse to any model of the transition process. Figure 3B shows the scanning curves for these molecules, measured at the same concentration (460 μM in total strands or 115 μM in junction). The resulting thermodynamic profiles for forming these junctions at 20 °C are also included in Table II. In each case, formation of the junction has a favorable free energy, resulting from partial compensation of a favorable enthalpy with an unfavorable entropy. Relative to J1, the substitution of a T–T mismatch to yield the T2 and T3 molecules results in a reduction of the overall favorable free energy by 3 and 4 kcal/mol, respectively. This reduction is dominated by the enthalpy contribution in each case. For the double-substituted mismatch molecule, T2T3, the observed changes in the thermodynamic parameters correspond nearly to the sum of the changes of the individual substitutions. The DSC profiles of the mismatched junctions have an additional feature of interest, a tendency to become asymmetric relative to the transition in J1 (Figure 3B). This is most apparent in the scanning curve for T3, which shows a shoulder with a transition at about 50 °C, above the T_m of intact junction.

(c) T–T Mismatches at the Branch Enhance Reactivity of Distal Residues in the Molecule. Duckett and Lilley (1991) classified several types of behavior of a mismatch at a branch, which depended on the nature of mismatch, the pH, and the neighboring sequence. The two T–T mismatches they studied were unable to assume a normal junction configuration, based on the patterns of their gel mobilities and the chemical reactivity of the T's at the substitution site to osmium tetraoxide (OsO_4) in Mg^{2+}. This reagent is active in oxidation of thymidylate residues in the unpaired state (Lilley & Palecek, 1984), reactivity being detected by sensitivity of the reacted site to piperidine-catalyzed hydrolysis. To determine the extent of conformational effects of the mismatches in our system, we measured the reactivity of these molecules to OsO_4 and to the purine-specific reagent, diethyl pyrocarbonate (Herr, 1985). Differential reactivity was monitored by the extent of cleavage in each strand of the mismatched species relative to that in the corresponding strand of J1 (Figure 4A). Figure 4B compares the patterns of reactivity of OsO_4 of the three mismatch-containing structures relative to the basal level in J1 as a control. Reactivity of this agent at each T within the mismatched site is clearly observed in all of the mismatched junctions. Enhanced reactivity can also be detected at other sites, implying that there is propagation of strain, or a change in the conformational equilibrium, altering the arms containing the mismatch as well as other arms. Figure 4C shows that a similar effect can be seen in the pattern of reactivity of the mismatched junctions to DEPC also: A12 in strand 3 becomes reactive in both T3 and T2T3, for example, but not in J1 or T2.

(d) Mismatches Enhance Reactivity of the Branch to MPE·Fe(II). A striking effect of exposing J1 to the reactive probe MPE·Fe(II) (Van Dyke & Dervan, 1983a,b) is the observation of enhanced reactivity of sites in the molecule near the branch (Guo et al., 1989). This increase in reactivity is detected most clearly at positions 9–11 in strand 1, 9 in strand 2, and 10 and 11 in strand 4 of J1 relative to fully duplex controls (Guo et al., 1989). These positions are indicated by a dot in Figure 5A. The effect is amplified significantly in the mismatched junctions, as shown in the densitometer traces in Figure 5A. If we refer intensity changes to the positions 5–7 or 14 in each strand, which tend to be invariant, the original positions of enhancement are each increased in the mismatched species. In addition, sites that are not seen to show enhanced scission in J1 respond in the mismatches: for example, position 9 in strands 3 and 4 shows clear enhancement. Since each panel was exposed for the same time, the relative intensities can be estimated from the traces shown: the increase in cutting is by a factor of 2–4-fold over the level in J1, while the affected sites in J1 itself are cleaved by 1.6–2-fold more than the corresponding positions in duplex controls (Guo et al., 1989). To establish that the enhanced reactivity of MPE is in fact due to preferential binding at the branch, we performed a footprint experiment using ethidium bromide, with the same ring system as in MPE, at a stoichiometry of 1:1 with junctions, and OsO_4 as a probe (data not shown). The results reveal a clear elimination of the enhanced reactivity of OsO_4 at the mismatch sites flanking the branch exclusively. As in the interaction of these molecules at the branch in J1, we infer that a selective interaction with the phenanthridine ring system occurs at the branch.

A question that arises is whether this behavior is peculiar to mismatches at a branch, as opposed to mismatches in duplex DNA. We addressed this by exposing two duplex mismatches corresponding to T2 and T3 (referred to as ds2-T and ds3-T),

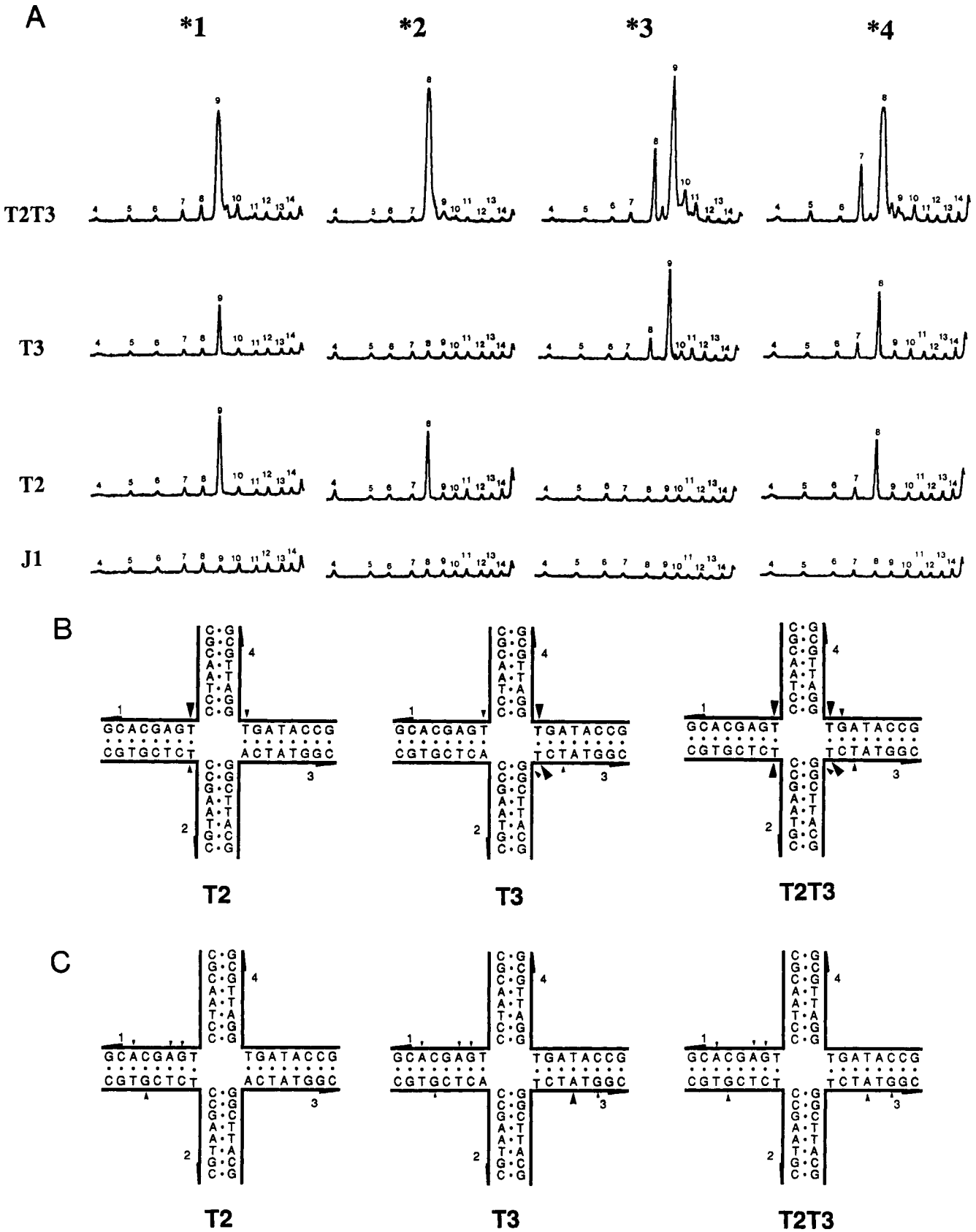

FIGURE 4: Chemical modification of junctions. (A) Scans of autoradiographs from osmium tetraoxide modification experiments. The reactions were carried out as described under Materials and Methods. Radioactively labeled strands are indicated by the number of the strand in the 5′ half. Note that the thymine bases in T–T mismatched junctions are hyperreactive. (B) Sites of preferential interaction with OsO_4 in T–T mismatched junctions compared to those in J1. The size of an arrow is a measure of the quantitative intensity of each responsive site. (C) Sites due to the differential modification by DEPC in T–T mismatched junctions relative to those in J1.

together with their intact control duplexes, to OsO_4 and to MPE·Fe(II). The results indicate no differential reactivity of ds2-T or ds3-T to OsO_4 (data not shown). However, clear evidence for selective interaction of MPE·Fe(II) at the mismatch is detected in both duplexes (Figure 6). The patterns of reactivity in this figure conform reasonably with those

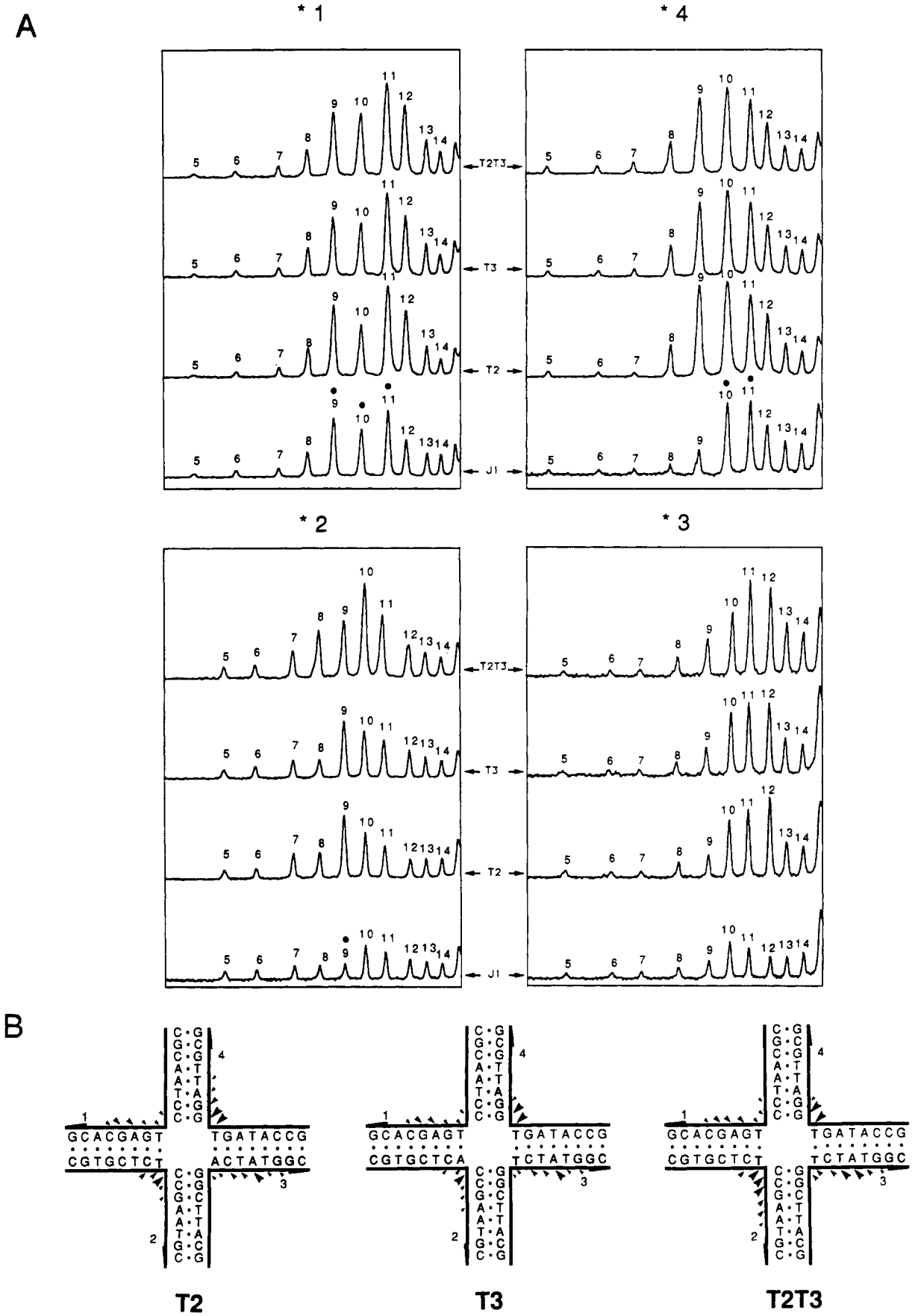

FIGURE 5: Cleavage of junctions by MPE·Fe(II). (A) Densitometric scans of the cleavage pattern of junctions due to MPE·Fe(II). Each quadrant of this figure corresponds to a given strand of junctions. Each panel of scans contains four scans, each corresponding to one of the junctions of this study. (●) indicates the positions of preferential cleavage in J1 relative to fully duplex controls (Guo et al., 1989). The branch point lies between positions 8 and 9 on each strand. Note that strong enhancements of cleavage near branch sites are seen in these T-T mismatched junctions relative to J1. (B) Sites of preferential cleavage by MPE·Fe(II) in T-T mismatched junctions compared to those in J1. The size of an arrow is a measure of the quantitative intensity of each responsive site.

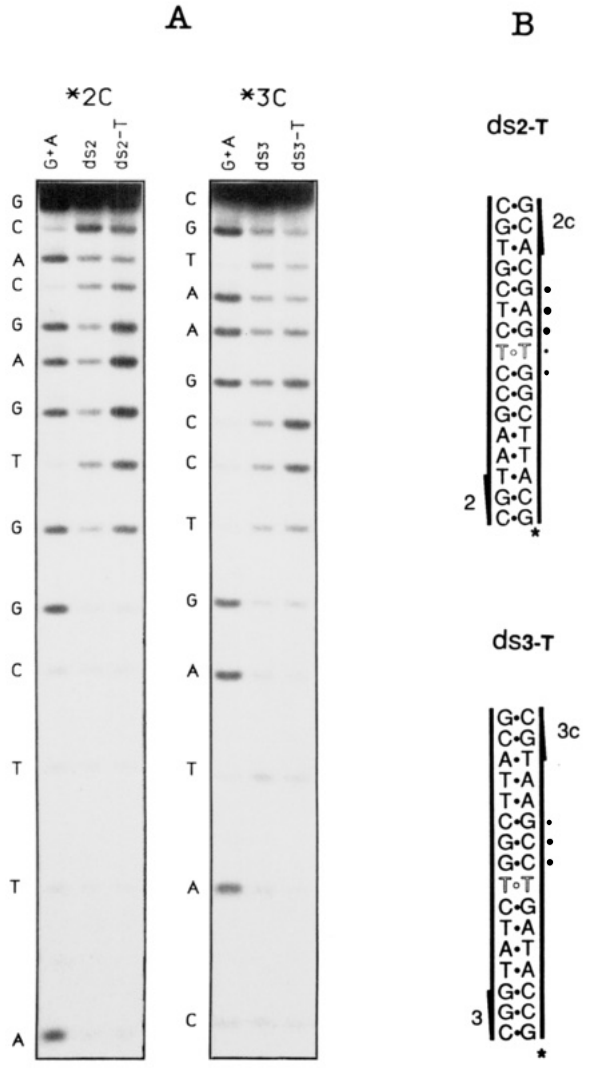

FIGURE 6: Cleavage of duplexes ds2, ds3, and their corresponding T–T mismatched duplexes ds2-T and ds3-T by MPE·Fe(II). (A) Autoradiograph of the gel. Duplexes 5′-labeled with ^{32}P in strands 2c and 3c, respectively, were cleaved by MPE·Fe(II) and electrophoresed on a sequencing gel alongside A+G sequence markers derived from the same radioactive strand. Radioactively labeled strands are indicated by the number of the strand in the 5′ half. (B) Sites of preferential cleavage in T–T mismatched duplexes by MPE·Fe(II) compared to those in the corresponding perfect duplexes. The size of a dot is a measure of the quantitative intensity of each responsive site.

anticipated for a single strong binding site for MPE·Fe(II), which is assumed to produce diffusible OH radicals that cleave the target DNA two to three bases from the actual binding site. No longer range effects comparable to the patterns seen in the mismatched junctions occur in duplexes, however.

DISCUSSION

We have described the thermodynamics and ligand binding properties of T–T mismatches at the branch site in an immobile DNA junction. The thermodynamic parameters indicate a substantial reduction in the enthalpy of complex formation from the single strands accompanying base mismatching at the branch. The difference between the DSC and van't Hoff enthalpies has been observed previously (Marky et al., 1987). One explanation that has been given for the greater magnitude of the van't Hoff heats is that the junctions involve more than 30 base pairs, reducing the dependence of T_m on concentration and amplifying the apparent enthalpy. Nevertheless, as seen in Table II, the heat differences determined from the van't Hoff and DSC enthalpies between J1 and the mismatched junctions are remarkably consistent. Each mismatch reduces the enthalpy of forming the junction by about 20 kcal/mol, and the two in T2T3 are roughly additive, 40 kcal/mol.

The reason for the asymmetry in the DSC profiles of the mismatched junctions is not obvious. A likely possibility for the presence of a "shoulder" above the transition temperatures of the mismatch molecules is a partial intramolecular refolding in the strand containing the mismatch. Deconvolution of the T3 transition, for example, is consistent with two monophasic transitions: a main transition with T_m = 40 °C and $\Delta H°_{cal}$ = 150 kcal/mol and a second with T_m = 50 °C and $\Delta H°_{cal}$ = 40 kcal/mol. The two transitions show only a weak dependence on strand concentration. The parameters for the latter transition are consistent with the formation of a hairpin molecule containing three or four base pairs in the stem, such as

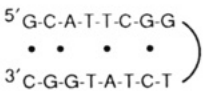

This interpretation is strengthened by the observation that the single strand with the T3 mismatch unfolds in a biphasic manner, with a transition near 40 °C (data not shown). Also, the shoulder appears clearly in UV thermal experiments monitored at 275 nm but not at 260 nm, consistent with formation of a G·C-rich structure. Formation and unfolding of such intermediates would not be expected to distort either the van't Hoff (determined from T_m–concentration dependence plots, not from shape analysis) or DSC thermodynamic parameters of the reaction in which four strands form a junction (Lu et al., 1992a,b).

Our second observation is that the presence of a T–T mismatch perturbs the structure at the junction and at sites several bases removed from the branch itself. This effect is not seen in the case of control duplex DNAs containing these mismatches (Figure 6). In addition, OsO_4 reacts with the mismatched T's flanking the branch in the junctions, but not with those at the site of mismatching in a duplex control [see also Cotton et al. (1988) and Bhattacharya and Lilley (1989)]. Thus, the mismatched T's at the branch act as more "open" species than those in a duplex. The T's become more accessible to a chemical probe; a significantly larger loss in enthalpy occurs in the former case than in duplexes (Tibanyenda et al., 1983; Aboul-Ela et al., 1985; Werntges et al., 1986). The magnitude of the enthalpy loss in the branched structure is about 20 kcal/mol for the T–T mismatch in these junctions; estimates for the corresponding enthalpy difference in a duplex are much lower, below 13 kcal/mol (Aboul-Ela et al., 1985). This additional enthalpic loss in the case of T–T mismatches at a junction might arise from a structural perturbation or from solvation or ionic differences at the branch, or both. For example, this enthalpy differnce would be enough to account for disruption of the postulated T–T wobble pairing seen in duplex DNA (Kouchakdjian et al., 1988). Such effects might influence the repair of mismatches and yield of recombinants in nonhomologous cases. In addition, there is some delocalized strain or conformation effect in the branched structure. Sites that are remote from the mismatch respond differently to MPE in the mismatched junctions (Figure 5), in all strands. This seems unlikely to reflect secondary redistribution of bound drug following the enhanced interaction at the branch (Dabrowiak et al, 1989), since no such effect is detected in the duplex case. A more likely explanation is that the mismatch

flanking the branch perturbs the conformational equilibrium in the junctions (Guo et al., 1991) or exerts a direct effect which induces or releases strain across the branch. The fact that OsO_4 and DEPC also show long-range effects indicates that this cannot be due to the methidium ligand itself, but is intrinsic to junctions containing T–T mismatches. Such long-range effects are of interest in terms of their ability to influence the substrate properties of a junction for resolvase enzymes, for example (Lu et al., 1991).

Finally, the interaction between the branch and intercalative ligands is strengthened. This is shown by the enhanced reactivity of sites near the branch to MPE in the mismatched junctions relative to those in J1. This behavior can be understood by means of a model in which the more open state of the mismatched pair at the branch facilitates interaction of the phenanthridine ring system of methidium over the relatively tighter structure in J1. Methidium interacts selectively at the mismatch site in the duplex control, consistent with this idea. If the transition state for ring insertion requires a distortional opening of the duplex, then weakening the stacking interactions and hydrogen bonding should enhance this rate and thereby favor binding. The reactivity of methidium at the T–T mismatch in the duplex and at the branch in a four-arm junction is enhanced by 2–4-fold over that at the corresponding sites in controls. If the chemical rate of scission is constant, these factors should apply to the binding affinity, and this would imply that selective binding to the mismatch is stronger than to the branch itself (Guo et al., 1989).

Thus, four-arm Holliday junctions formed from nonhomologous strands respond differently to drugs or other ligands from those formed from homologous pairs. The details of the interactions can be expected to vary depending on the nature of the mismatched bases and context, based on precedents from duplex DNA as well as junctions (Duckett & Lilley, 1991). Mismatched sites can differ in important respects from normal paired DNA: the detailed pairing, stability, local dimensions of the helix, and its charge and hydration have all been seen to differ from those of B-DNA (Kneale et al., 1985; Prive et al., 1987; Brown et al., 1990). The T–T mismatches we have studied have distinctly different effects on the stability and conformation of junctions than they do in duplex DNA. The efficiency of duplex DNA repair depends both on the identity of the mismatch and the flanking sequence (Kramer et al., 1984), and it can be anticipated that these factors will influence the outcome of recombinational events also (Nunes-Duby et al., 1987; deMassy et al., 1989; Nash & Robertson, 1989).

ACKNOWLEDGMENT

This research was supported by NIH Grants CA24101 and GM42223.

REFERENCES

Aboul-Ela, F., Koh, D., Tinoco, I., Jr., & Martin, F. H. (1985) *Nucleic Acids Res. 13*, 4811–4824.

Bhattacharya, A., & Lilley, D. M. J. (1989) *J. Mol. Biol. 209*, 583–597.

Brown, T., Leonard, G. A., Booth, E. D., & Kneale, G. (1990) *J. Mol. Biol. 212*, 437–440.

Cantor, C., Warshaw, M. W., & Shapiro, H. (1970) *Biopolymers 9*, 1059–1077.

Caruthers, M. H. (1982) in *Chemical and Enzymatic Synthesis of Gene Fragments* (Gassen, H. G., & Lang, A., Eds.) pp 71–79, Verlag Chemie, Weinheim.

Cooper, J. P., & Hagerman, P. J. (1987) *J. Mol. Biol. 198*, 711–719.

Cooper, J. P., & Hagerman, P. J. (1989) *Proc. Natl. Acad. Sci U.S.A. 86*, 7336–7340.

Cotton, R. G. H., Rodrigues, N. R., & Campbell, R. D. (1988) *Proc. Natl. Acad. Sci. U.S.A. 85*, 4397–4401.

Dabrowiak, J. C., Ward, B., & Goodisman, J. (1989) *Biochemistry 28*, 331–3322.

deMassy, B., Dorgai, L., & Weisberg, R. A. (1989) *EMBO J. 9*, 1591–1599.

Duckett, D. R., & Lilley, D. M. J. (1991) *J. Mol. Biol. 221*, 149–161.

Guo, Q., Seeman, N. C., & Kallenbach, N. R. (1989) *Biochemistry 28*, 2355–2359.

Guo, Q., Lu, M., Seeman, N. C., & Kallenbach, N. R. (1990) *Biochemistry 29*, 570–578.

Guo, Q., Lu, M., & Kallenbach, N. R. (1991) *Biopolymers 31*, 359–372.

Herr, W. (1985) *Proc. Natl. Acad. Sci. U.S.A. 82*, 8009–8013.

Kallenbach, N. R., Ma, R.-I., & Seeman, N. C. (1983) *Nature 305*, 829–831.

Kneale, G., Brown, T., Kennard, O., & Rabinovitch, D. (1985) *J. Mol. Biol. 186*, 805–814.

Kouchakdjian, M., Li, B. F. L., Swann, P. F., & Patel, D. J. (1988) *J. Mol. Biol. 202*, 139–155.

Kramer, B., Kramer, W., & Fritz, H.-J. (1984) *Cell 31*, 879–887.

Lilley, D. M. J., & Palecek, E. (1984) *EMBO J. 3*, 1187–1192.

Lu, M., Guo, Q., Studier, F. W., & Kallenbach, N. R. (1991) *J. Biol. Chem. 266*, 2531–2536.

Lu, M., Guo, Q., & Kallenbach, N. R. (1992a) *Crit. Rev. Biochem. Mol. Biol. 27*, 157–190.

Lu, M., Guo, Q., Marky, L. A., Seeman, N. C. & Kallenbach, N. R. (1992b) *J. Mol. Biol. 223*, 781–789.

Marky, L. A. & Breslauer, K. J. (1987) *Biopolymers 26*, 1601–1620.

Marky, L. A., Kallenbach, N. R., McDonough, K. A., Seeman, N. C., & Breslauer, K. J. (1987) *Biopolymer 26*, 1621–1634.

Maxam, A. M., & Gilbert, W. (1980) *Methods Enzymol. 65*, 499–560.

Nash, H. A., & Robertson, C. A. (1989) *EMBO J. 8*, 3523–3533.

Nunes-Duby, S. E., Matsumoto, L., & Landy, A. (1987) *Cell 50*, 779–788.

Prive, G. G., Heinemann, U., Chandrasegaran, S., Kan, L.-S., Kopka, M. L., & Dickerson, R. E. (1987) *Science 238*, 498–504.

Tibanyenda, N., deBruin, S. H., Haasnoot, C. A., van der Marel, G. A., van Boom, J. H., & Hilbers, C. W. (1983) *Eur. J. Biochem. 139*, 19–25.

van Dyke, M. W., & Dervan, P. B. (1983a) *Cold Spring Harbor Symp. Quant. Biol. 47*, 346–353.

van Dyke, M. W., & Dervan, P. B. (1983b) *Nucleic Acids Res. 11*, 5555–5567.

von Kitzing, E., Lilley, D. M. J., & Diekmann, S. (1990) *Nucleic Acids Res. 18*, 2671–2683.

Werntges, H., Steger, G., Riesner, D., & Fritz, H.-J. (1986) *Nucleic Acids Res. 14*, 3773–3790.